

Dynamical Properties of a Room Temperature Ionic Liquid: Using Molecular Dynamics Simulations to Implement a Dynamic Ion Cage Model

Maolin Sha^{*,†,‡}, Xiaohang Ma[†], Na Li[¶], Fabao Luo[¶], Guanglai Zhu[¶], and
Michael D. Fayer^{*,‡}

[†]Department of Physics and Materials Engineering, Hefei Normal University, Hefei
230061, China

[‡] Department of Chemistry, Stanford University, Stanford, California 94305, United
States.

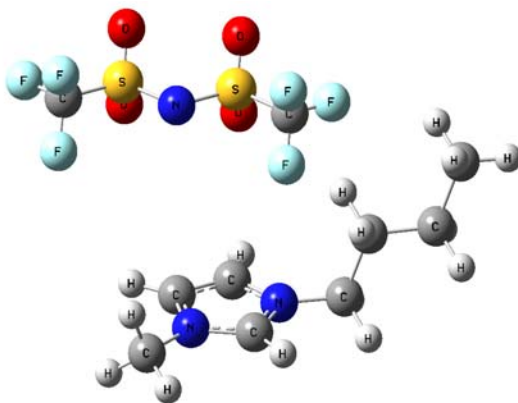
[¶]Department of Chemistry and Chemical Engineering, Hefei Normal University, Hefei
230061, China

[¶]Institute of Atomic and Molecular Physics, Anhui Normal University, Wuhu 241000,
China.

*Email: franksha@aliyun.com; fayer@stanford.edu. Phone: 650 723-4446.

Supporting Material

1. Molecular structure of [Bmim][NTf₂]



2. Density

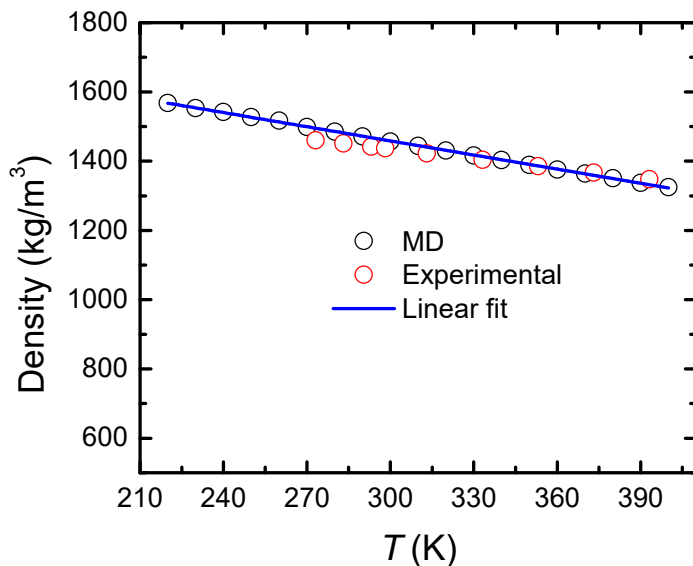


Figure S1. The temperature-dependent mass densities of BmimNTf₂. The experimental densities of [Bmim][NTf₂] are from Hamidova et al.¹

Figure S1 displays the temperature dependent mass densities of [Bmim][NTf₂] from our MD simulations. The good linear behavior of the mass density with increasing temperature shows that the force field can accurately simulate the structural properties of the IL [Bmim][NTf₂].

3. Diffusion coefficients

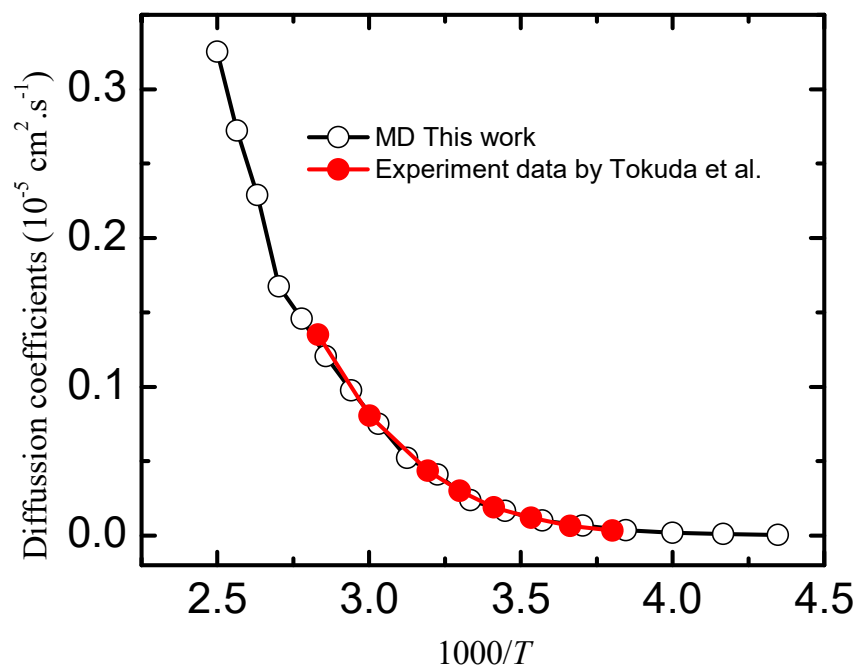


Figure S2. The temperature-dependent diffusion coefficients of [Bmim][NTf₂]. The experimental data are from Tokuda et al.²

4. Diffusion and rotational dynamics comparison between the nonpolarizable force field and a polarizable force field

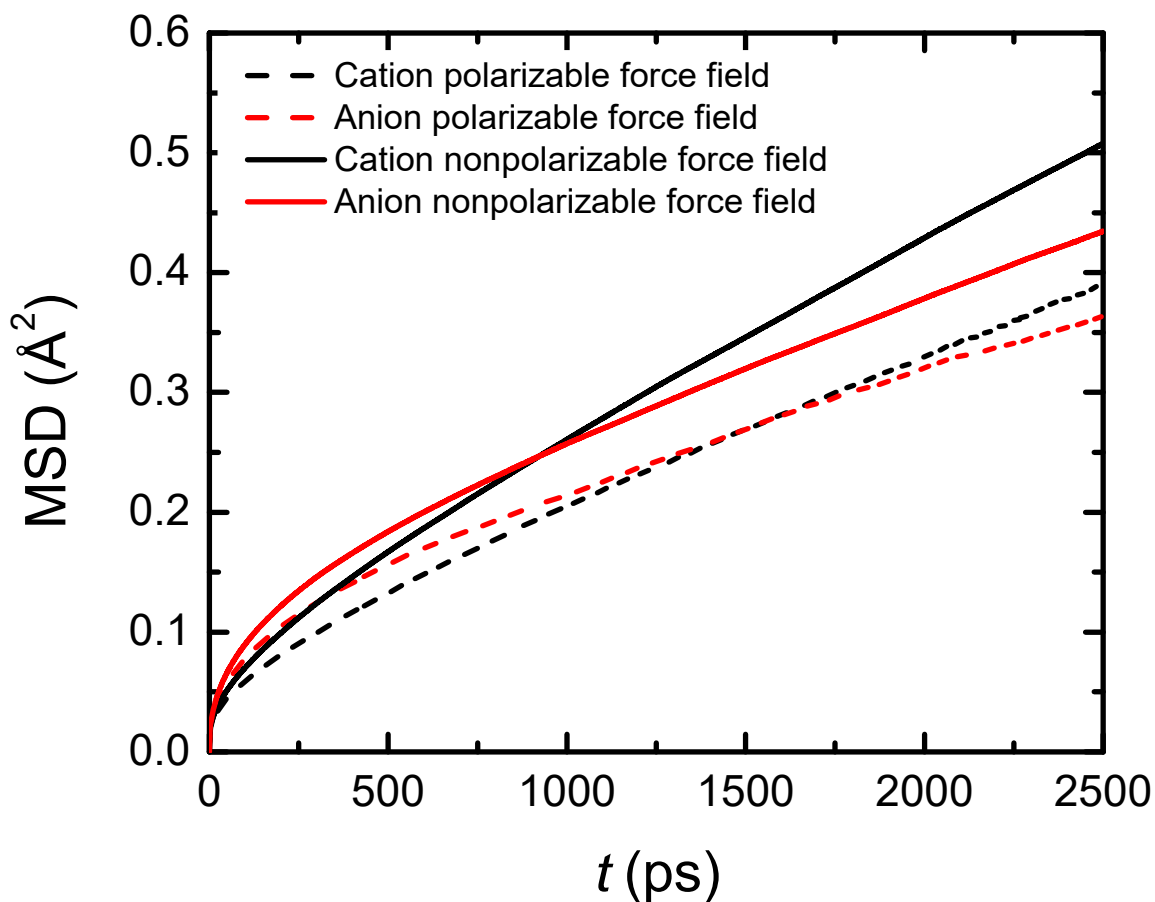


Figure S3. The comparison of the mean square displacement (MSD) of the IL cation and anion between the force field developed by Köddermann et al.³ and recent polarizable force field at 300 K. The polarizable force field parameters were from Choi, et . al.⁴

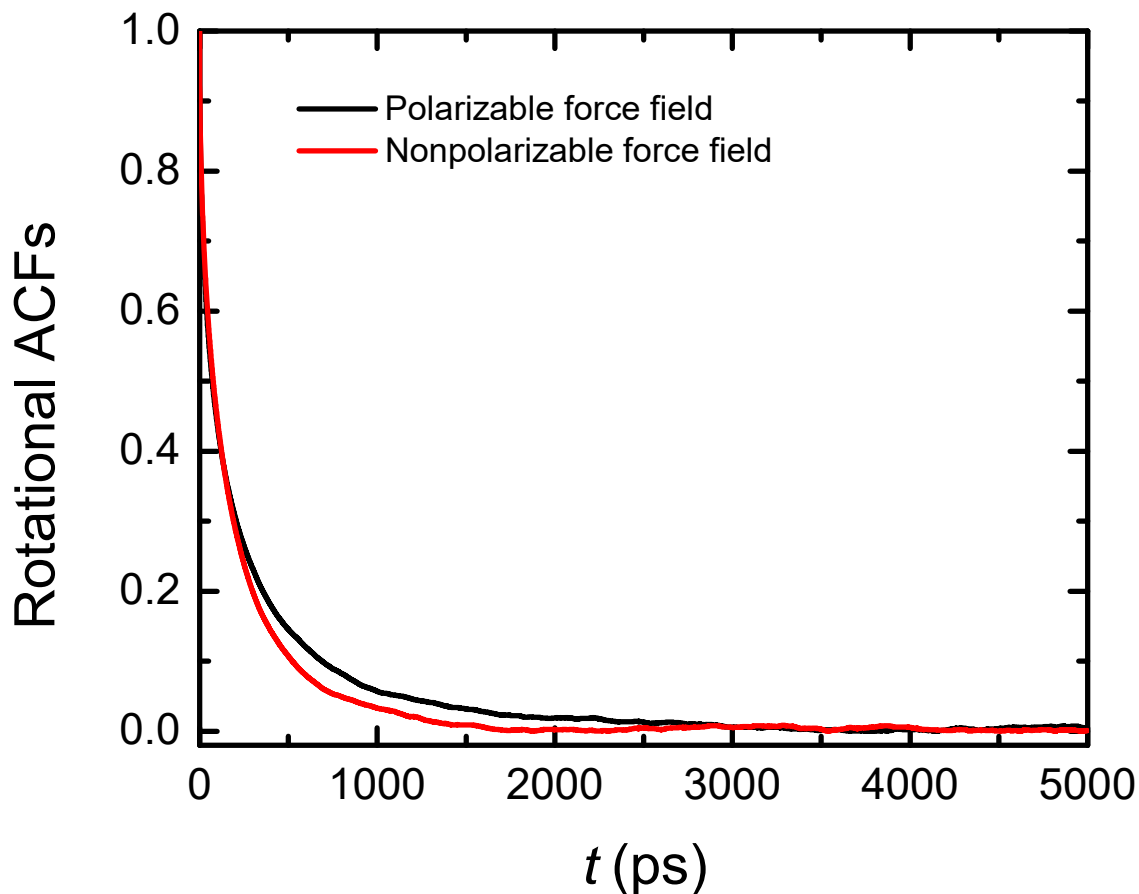


Figure S4. The comparison of the rotational autocorrelation functions (ACF) of the vertical direction of the IL cation ring between the force field developed by Köddermann et al.³ and recent polarizable force field at 300 K. The polarizable force field parameters were from Choi, et . al.⁴

In order to validate the reasonability of our force field, we calculated the diffusion and rotational dynamics by the first-principles-based polarizable force field,⁴ which is from the symmetry-adapted perturbation theory, and compared it to our force field's results. In both the figure S3 and S4, the differences of dynamic properties between our force field and polarizable force field are very small. For example, the diffusion coefficients in the polarizable force field at 300 K are $D_{cation} = 0.0213 \times 10^{-5} \text{ cm}^2 \cdot \text{s}^{-1}$, $D_{anion} = 0.0174 \times 10^{-5} \text{ cm}^2 \cdot \text{s}^{-1}$. Our force field's results are $D_{cation} = 0.0237 \times 10^{-5} \text{ cm}^2 \cdot \text{s}^{-1}$, $D_{anion} = 0.0179 \times 10^{-5} \text{ cm}^2 \cdot \text{s}^{-1}$, slightly faster than the polarizable force field. The same trend can be seen in the rotational dynamics in figure S4. Usually, the computation expense of the polarizable force field is about 10 times slower than the nonpolarizable force field. Hence, our force field shows a good efficiency and precision to reproduce the dynamic properties of IL [Bmim][Ntf₂].

5. Mean square displacement

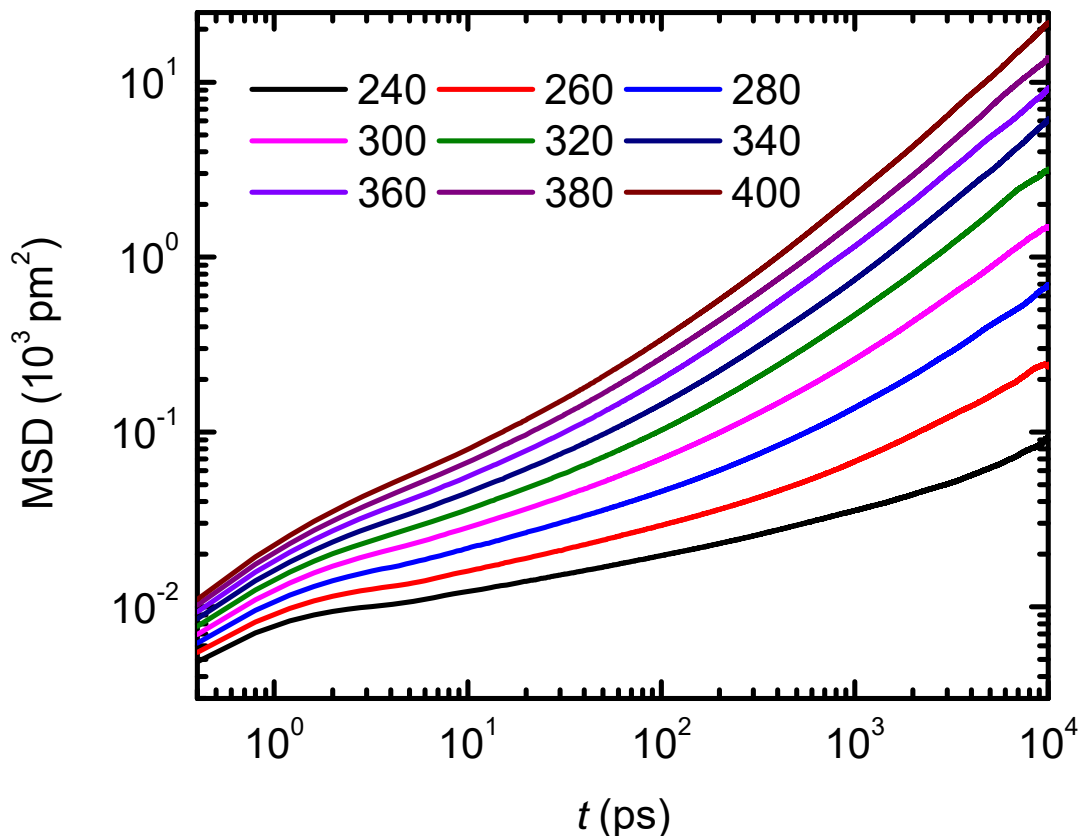


Figure S5. The mean square displacement (MSD) of the IL cation at different temperatures.

The MSD curves in Figure S5 initially show a super-diffusion behavior, which might arise from ballistic motion. Then there is typical sub-diffusive behavior, i.e. a fractional power law exponent from ~ 100 ps to approximately a nanosecond due to the cage effect, and finally a gradual change into a normal linear relationship at long time on the log plot. These super-diffusive and sub-diffusive behaviors were also confirmed previously by experiments and molecular dynamics simulations.^{5,6}

6. The temperature dependence of the rotational autocorrelation functions

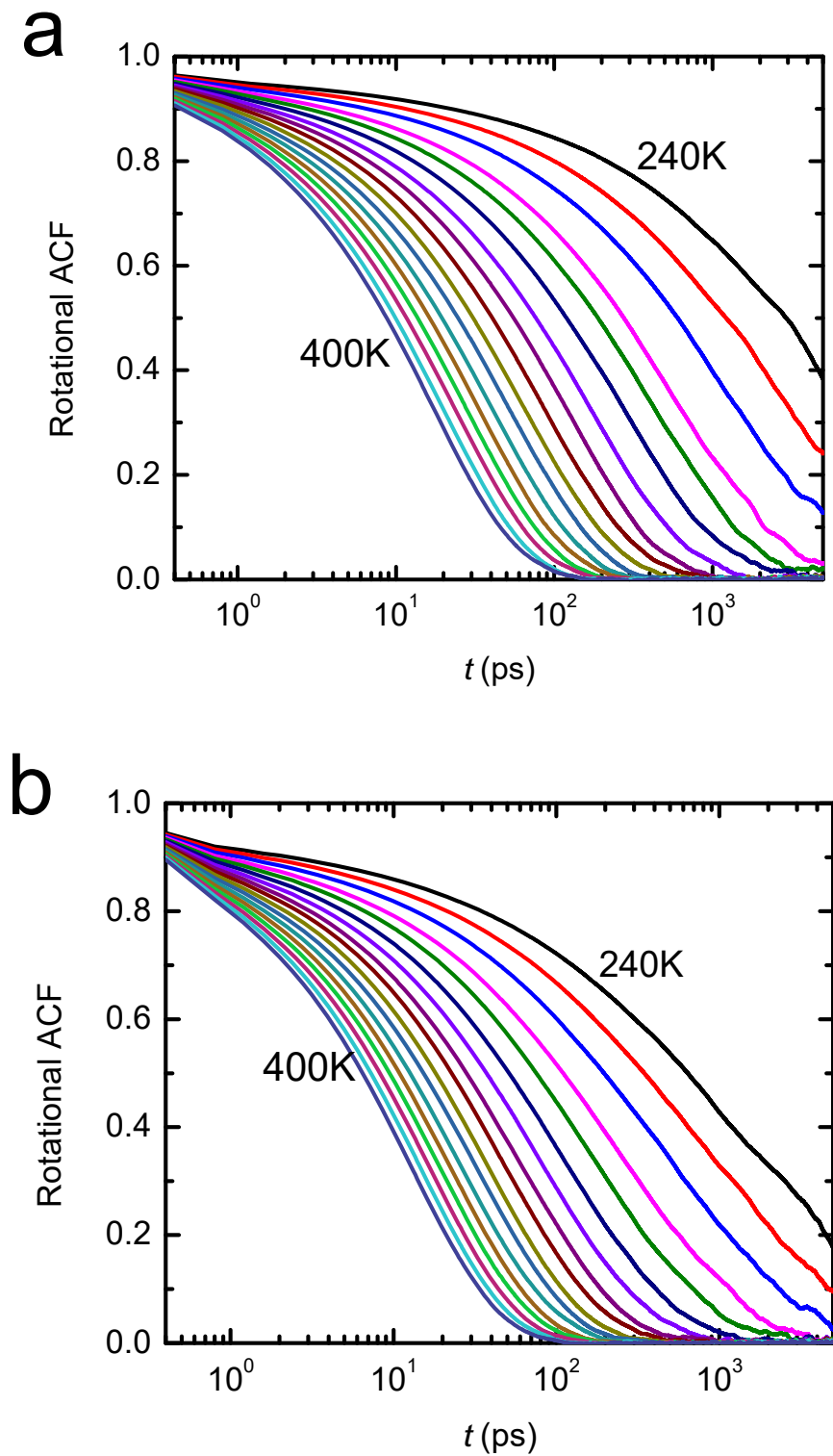


Figure S6. The temperature dependent rotational autocorrelation function $C_1(t)$ for (a) the cation and (b) anion. The rotational axis of the cation is perpendicular to the imidazolium ring. We chose the S-S vector as the rotational axis of the anion.

7. The hydrodynamic model calculations

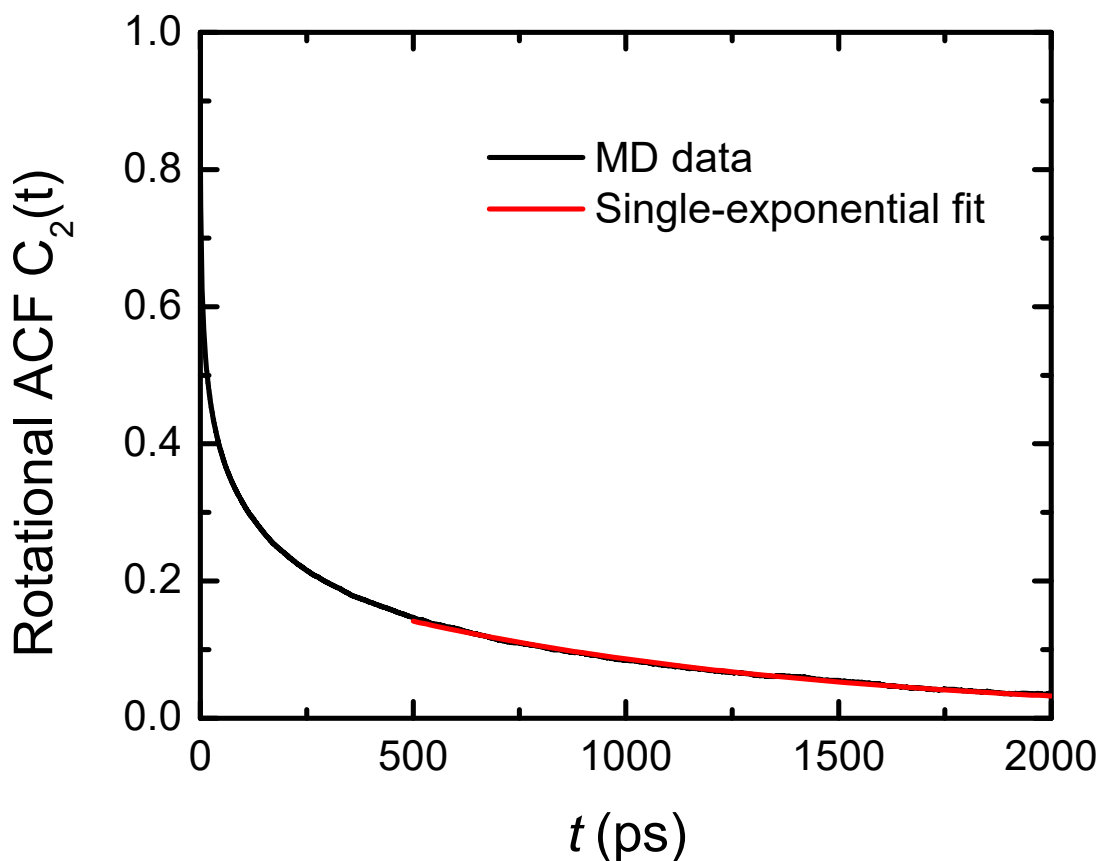


Figure S7. The rotational autocorrelation function $C_2(t)$ of the IL cation at 300 K. The rotational direction is normal to imidazolium ring. A long-time single-exponential fit is shown in red color.

There are two ways to obtain the orientational relaxation time from the rotational autocorrelation function (ACF) $C_2(t)$ (see figure S7). In the molecular dynamic simulation, the various relaxation times are usually calculated by integrating the decay curves. When we integrated the ACF $C_2(t)$, $\tau_{R2} = \int_0^{\infty} C_2(t) dt$, we obtained a value of the orientational relaxation time of 244 ps. However, this integration method has a deficiency, i. e., it is heavily dependence on the short-time decay of the ACF. We know that the rotational ACF at short time is related to not only the rotational contribution but also the translational or collision contribution of the molecule. Hence, it is common to use a single-exponential function to fit the ACF for the long time decay in experiments. When we fitted the long time decay of the ACF $C_2(t)$ in Figure S5, with a single-exponential function (from 500 ps to 2000 ps), the fit function is $Y = 0.23e^{(-t/1015)}$. Hence, the rotational lifetime for a single-exponential fit at long time is ~ 1015 ps. The viscosity of the

[Bmim][NTf₂] at 300 K is about 69 cP.⁷ The long-axis value is 9.92 Å and short-axis is 4.24 Å from a Gaussian 09 calculation. Hence, the ratio ρ is ~ 0.43 . According to the tabulated friction coefficients for prolate spheroid,^{8,9} the λ value is ~ 4.17 .

If we use the integrated rotational lifetime, the calculated hydrodynamics volume of the cation is about 0.021 nm³ at 300 K, which is about 9 times smaller than the cation volume value 0.196 nm³¹⁰ and 7 times smaller than the cation Van der Waals volume 0.142 nm³.¹¹ If we use the single-exponential fit time 1015.4ps as rotational lifetime, the calculated hydrodynamic volume is 0.088 nm³, which is also 2.2 times smaller than the cation volume and 1.6 times smaller than the cation Van der Waals volume.

8. The relationship between the rotational lifetime and the cage lifetime

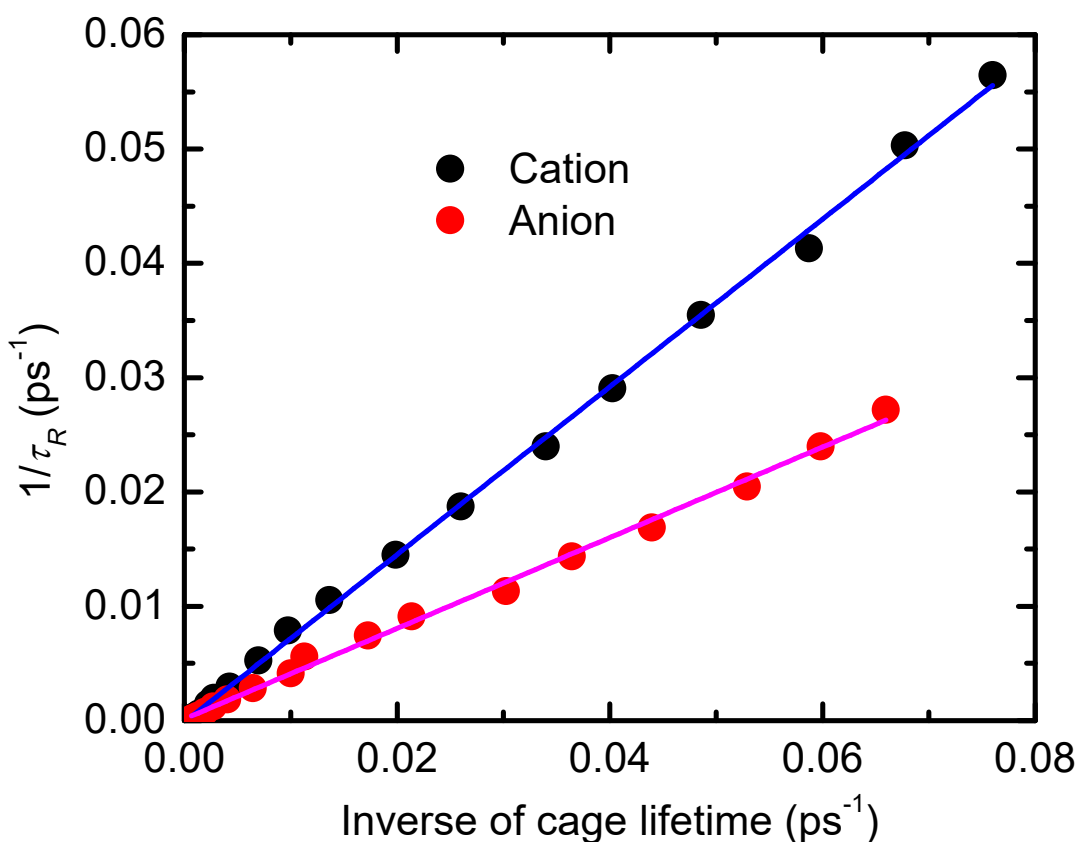


Figure S8. The linear relationship between the rotational lifetimes and the cage lifetimes.

Figure S8 shows a linear relationship between the rotational lifetimes and the cage lifetimes.

These results demonstrate that the rotational motion is directly related to the cage jump time and the diffusion dynamics. Hence, a possible diffusion mechanism was suggested to explain the diffusion dynamics, i.e. an ion rotates within a counter ion cage, and then jumps from an ion cage to another ion cage. The diffusion dynamics are heavily coupled to the rotational motion and the cage jump dynamics.

9. The relationship between the coordination number of the ion cage and the temperature

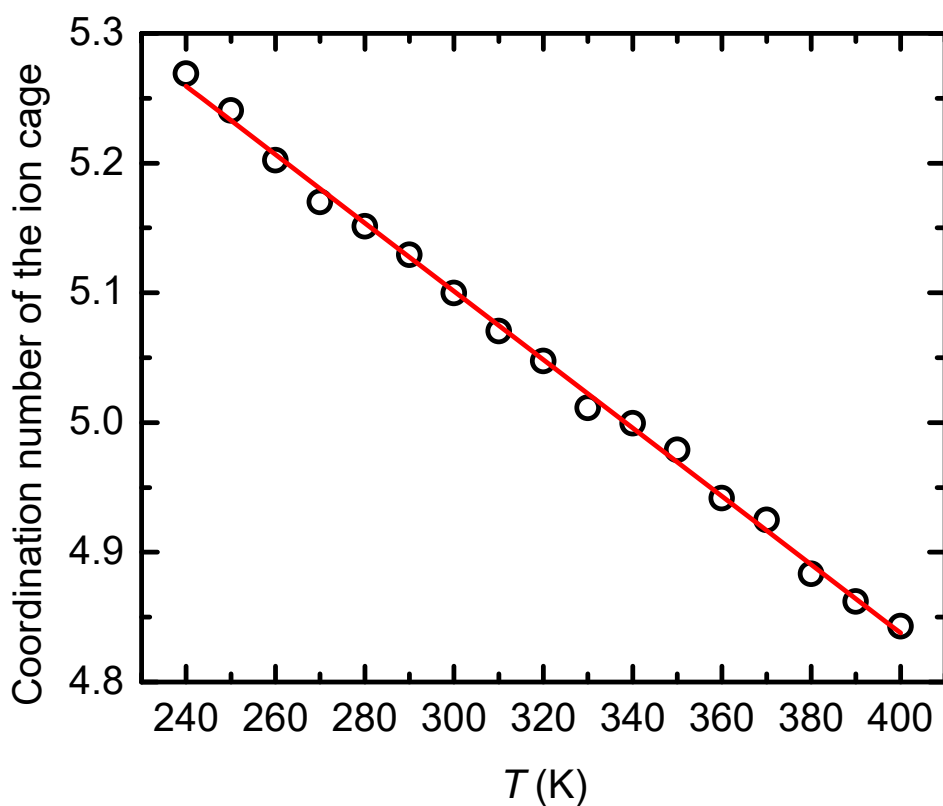


Figure S9. The temperature dependent coordination number of the ion cage.

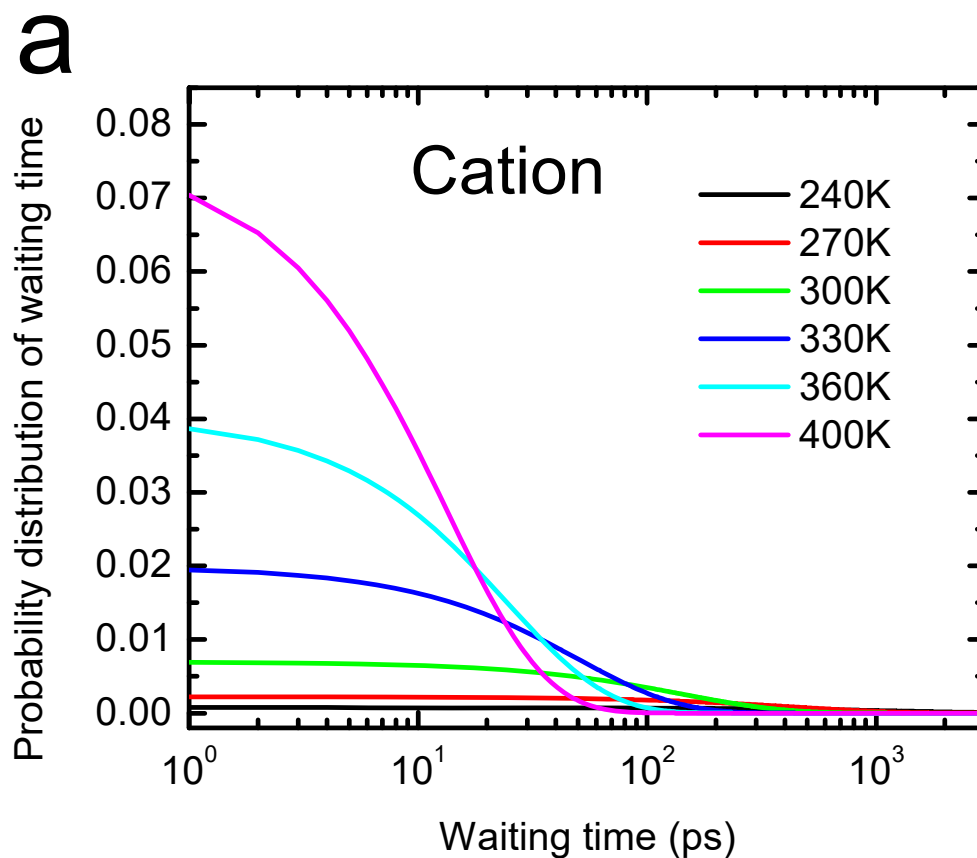
Figure S9 shows a good linear relationship between the coordination number of the ion cage and the temperature. Thus, the increase in the temperature only induces a mild linear decrease of the coordination number of the ion cage rather.

10. The VFT fit parameters and the fit parameters of equation 6

Table S1. The VFT fit parameters and the fit parameters of equation 6 in the paper

$Y = A \cdot \exp(B/(T-T_0))$	A	B	T_0
Cation ISF lifetime	0.064	942.05	158.4
Anion ISF lifetime	0.206	850.32	162.84
Cation diffusion	11.28	-884.85	154.54
Anion diffusion	11.24	-927.78	152.2
Cation rotation lifetime	0.49	868.17	155.4
Anion rotation lifetime	0.72	686.99	161.1
$Y = A \cdot \exp(B/(C-1/X))$	A	B	C
Coordinate number/cation	18.7	0.11	0.18
Coordinate number/anion	17.2	0.12	0.18

11. Probability distribution of waiting times in the ion cage



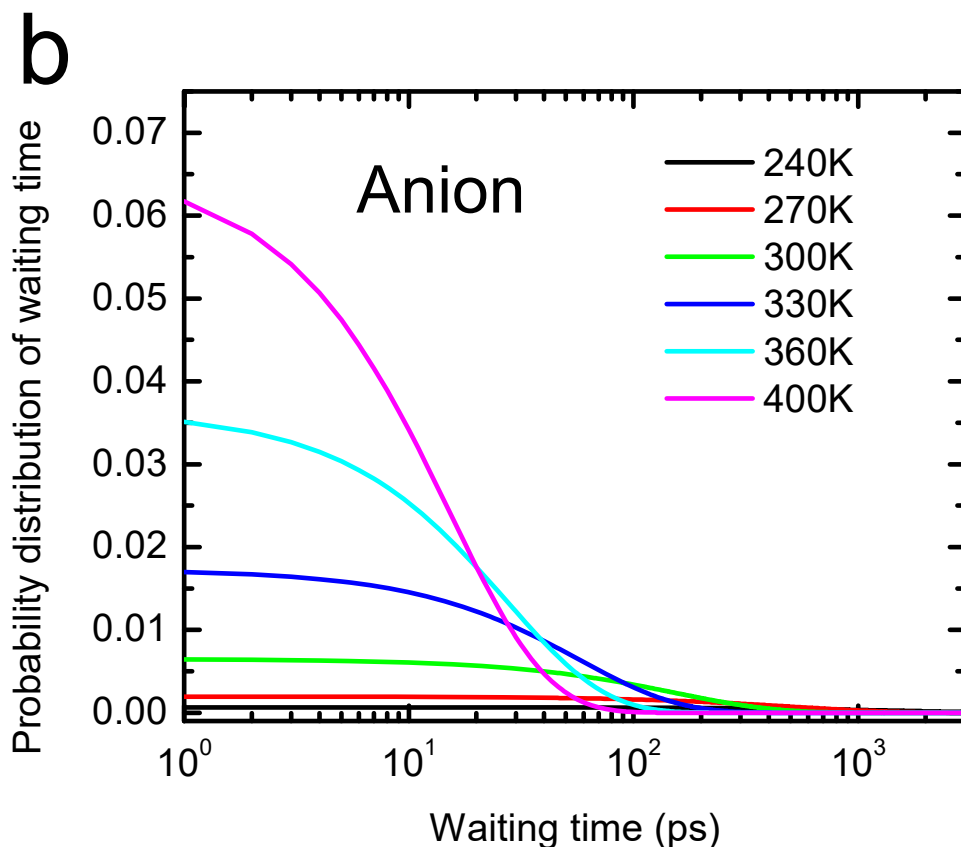


Figure S10. The temperature dependent probability distribution of waiting times in the ion cage. (a) cation (b)anion.

Based on the random walk model, the waiting time can be described by $(t) = \frac{1}{\tau_c} e^{-\frac{t}{\tau_c}}$. Here, τ_c is the lifetime of the ion cage. Hence, the probability distribution of waiting times is a single-exponential decay. At low temperature, the values of the lifetimes of the ion cage are very long; the probability distribution decays very slowly, a significant probability exists for more than a nanosecond. At high temperature, the waiting times are very short, the decays occurring tens to hundreds of picoseconds.

References

- (1) Hamidova, R.; Kul, I.; Safarov, J.; Shahverdiyev, A.; Hassel, E. Thermophysical properties of 1-butyl-3-methylimidazolium bis(trifluoromethylsulfonyl)imide at high temperatures and pressures, *Braz. J. Chem. Eng.* **2015**, *32*, 303-316.
- (2) Tokuda, H.; Tsuzuki, S.; Susan, M. A. B. H.; Hayamizu, K.; Watanabe, M. Physicochemical

properties and structures of room-temperature ionic liquid. 3. Variation of cationic structures, *J. Phys. Chem. B* **2006**, *110*, 19593-19600.

(3) T. Köddermann, D. Paschek, and R. Ludwig, *ChemPhysChem* **8**, 2464 (2007).

(4) Choi, E.; McDaniel, J. G.; Schmidt, J. R.; Yethiraj, A. First-principles, physically motivated force field for the ionic liquid [Bmim][BF₄], *J. Phys. Chem. Lett.*, **2014**, *5*, 2670-2674.

(5) Del Pópolo, M. G.; Voth, G. A. On the structure and dynamics of ionic liquids, *J. Phys. Chem. B*, **2004**, *108*, 1744-1752.

(6) Casalegno, M.; Raos, G.; Appetecchi, G. B.; Passerini, S.; Castiglione, F.; Mele, A. From nanoscale to microscale: crossover in the diffusion dynamics within two pyrrolidinium-based ionic liquids, *J. Phys. Chem. Lett.*, **2017**, *8*, 5196-5202.

(7) Huddleston, J. G.; Visser, A. E.; Reichert, W. M.; Willauer, H. D.; Broker, G. A. and Rogers, R. D., Characterization and comparison of hydrophilic and hydrophobic room temperature ionic liquids incorporating the imidazolium cation, *Green Chem.*, **2001**, *3*, 6164.

(8) Hu, C. and Zwanzig, R. Rotational friction coefficients for spheroids with the slipping boundary condition, *J. Chem. Phys.* **1974**, *60*, 4354.

(9) Sension, R. J. and Hochstrasser, R. M. Comment on: Rotational friction coefficients for ellipsoids and chemical molecules with slip boundary conditions, *J. Chem. Phys.* **1993**, *98*, 2490.

(10) Preiss, U. P. R. M.; Slattery, J. M. and Krossing, I. In silico prediction of molecular volumes, heat capacities, and temperature-dependent densities of ionic liquids, *Ind. Eng. Chem. Res.*, **2009**, *48*, 2290-2296.

(11) Beichel, W.; Eiden, P. and Krossing, I. Establishing consistent van der Waals volumes of polyatomic ions from crystal structures, *ChemPhysChem*, **2013**, *14*, 3221-3226.